



A zipped-helix cap potentiates HAMP domain control of chemoreceptor signaling

Caralyn E. Flack^a and John S. Parkinson^{a,1}

^aBiology Department, University of Utah, Salt Lake City, UT 84112

Edited by Caroline S. Harwood, University of Washington, Seattle, WA, and approved March 1, 2018 (received for review December 11, 2017)

Environmental awareness is an essential attribute for all organisms. The chemotaxis system of *Escherichia coli* provides a powerful experimental model for the investigation of stimulus detection and signaling mechanisms at the molecular level. These bacteria sense chemical gradients with transmembrane proteins [methyl-accepting chemotaxis proteins (MCPs)] that have an extracellular ligand-binding domain and intracellular histidine kinases, adenylate cyclases, methyl-accepting proteins, and phosphatases (HAMP) and signaling domains that govern locomotor behavior. HAMP domains are versatile input–output elements that operate in a variety of bacterial signaling proteins, including the sensor kinases of two-component regulatory systems. The MCP HAMP domain receives stimulus information and in turn modulates output signaling activity. This study describes mutants of the *Escherichia coli* serine chemoreceptor, Tsr, that identify a heptad-repeat structural motif (LLF) at the membrane-proximal end of the receptor signaling domain that is critical for HAMP output control. The homodimeric Tsr signaling domain is an extended, antiparallel, four-helix bundle that controls the activity of an associated kinase. The N terminus of each subunit adjoins the HAMP domain; the LLF residues lie at the C terminus of the methylation-helix bundle. We found, by using *in vivo* Förster resonance energy transfer kinase assays, that most amino acid replacements at any of the LLF residues abrogate chemotactic responses to serine and lock Tsr output in a kinase-active state, impervious to HAMP-mediated down-regulation. We present evidence that the LLF residues may function like a leucine zipper to promote stable association of the C-terminal signaling helices, thereby creating a metastable helix-packing platform for the N-terminal signaling helices that facilitates conformational control by the HAMP domains in MCP-family chemoreceptors.

bacterial chemotaxis | sensory adaptation | signal transduction | MCP

Success in the biological world depends on the ability to sense and respond adaptively to environmental cues. Bacteria use two extensively studied stimulus-response systems to cope with a wide variety of selective challenges: two-component signaling pathways that mediate changes in gene expression and chemotaxis signaling pathways that control locomotor behaviors (1–4). Bacterial signaling systems offer powerful models for exploring molecular mechanisms of stimulus detection and response. The simplest two-component pathways comprise a transmembrane sensor kinase that detects an environmental stimulus and a cytoplasmic response regulator that produces an adaptive change in gene expression, enabling the cell, for example, to metabolize a newfound nutrient or to inactivate a toxic compound. The simplest chemotaxis pathways comprise a set of transmembrane chemoreceptors, known as methyl-accepting chemotaxis proteins (MCPs), and six or more cytoplasmic proteins that transmit receptor signals to the locomotor machinery. This sensory system enables cells to track chemical gradients, an ability that can lead to more complex behaviors such as biofilm formation or host colonization (5–9).

Sensor kinases and MCP molecules have similar architectures: both are typically homodimeric, with membrane-spanning helices connecting their extracellular sensing domain to their cytoplasmic signaling domain. Many sensor kinases and MCPs contain a

histidine kinases, adenylate cyclases, methyl-accepting proteins, and phosphatases (HAMP) domain on the cytoplasmic side of the cell membrane between transmembrane helices and the output signaling domain. HAMP domains are versatile signaling modules that negotiate the conformational interactions between input and output signaling elements. A variety of HAMP signaling mechanisms have been proposed, from discrete two-state models (10–15) to dynamics-based models involving a range of metastable conformational states (16–20). In essence, however, all HAMP signaling models posit stimulus-induced changes in the packing stability or geometry of the four-helix HAMP bundle. HAMP signaling shifts, in turn, appear to modulate the packing interactions or orientation of adjoining output domain helices, which are coupled in structural opposition to the C-terminal HAMP helices through an intervening phase stutter (16, 18, 21, 22). The oppositional coupling between HAMP and the signaling elements it controls may poise receptors so that small changes in free energy upon ligand binding can propagate meaningful conformational or dynamics changes throughout the molecule (3, 17, 18, 23, 24).

The HAMP domains of sensor kinases and MCP chemoreceptors seem to employ a common mechanism for input–output control (18). However, the output domains of sensor kinases and MCPs have rather different structures. The catalytic domains of sensor kinases are globular with a helical extension in each subunit connected to the HAMP domain. HAMP conformational changes modulate kinase activity by manipulating those control helices (1, 2, 25, 26). In contrast, the output signaling domains of chemoreceptors form a long antiparallel, four-helix bundle, with a direct HAMP connection to the N-terminal helix of each subunit (Fig. 1). How might a HAMP domain manipulate the four-helix bundle of an MCP signaling domain to modulate the receptor's output state?

Significance

The ability to sense and respond adaptively to environmental changes is central to all forms of life. The bacterial chemotaxis system offers an ideal model system for the study of transmembrane and intracellular signaling mechanisms at the molecular level. Our studies of the *Escherichia coli* serine chemoreceptor have identified an evolutionarily conserved structural motif that is essential for control of receptor signal output by HAMP (histidine kinases, adenylate cyclases, methyl-accepting proteins, and phosphatases) domains, the versatile input–output devices that operate in a variety of bacterial signaling proteins.

Author contributions: C.E.F. and J.S.P. designed research; C.E.F. performed research; C.E.F. and J.S.P. analyzed data; and C.E.F. and J.S.P. wrote the paper.

The authors declare no conflict of interest.

This article is a PNAS Direct Submission.

Published under the PNAS license.

¹To whom correspondence should be addressed. Email: parkinson@biology.utah.edu.

This article contains supporting information online at www.pnas.org/lookup/suppl/doi:10.1073/pnas.1721554115/-DCSupplemental.

Published online March 26, 2018.

The cytoplasmic signaling domains of MCP molecules fall into different length classes defined by the number of coiled-coil heptad repeats they contain (31). *E. coli* receptors belong to the 36H class, with 18 heptads in the N-helices and 18 in the C-helices. Strikingly, most MCP subtypes (34H, 36H, 38H, 40H, 44H) contain three highly conserved residues in the C-terminal helices of the MH cap: two leucines and a phenylalanine, each spaced seven residues apart in *d* heptad positions for coiled-coil packing (Fig. 1*B*). This LLF residue motif is a defining feature of MCPs (31), but its function has never been explored to our knowledge. In this study, we characterize the signaling properties of Tsr LLF mutants and show that this motif potentiates an MH cap structure that facilitates HAMP signaling control. Our findings provide molecular insight into the mechanistic basis for HAMP signaling transactions in chemoreceptors.

Results

Mutational Analysis of the Tsr LLF Motif. To explore the signaling roles of the LLF motif residues in Tsr, we constructed and characterized a series of mutant receptors with all possible single amino acid replacements at Tsr residues L501, L508, and F515. Mutant receptors, hereafter designated LLF*, were generated by all-codon mutagenesis of Tsr expression plasmid pRR53 (32, 33). The mutant plasmids were then tested in a receptor-less host strain (UU2612) for their ability to support serine chemotaxis. We found that most LLF* receptors failed to support serine chemotaxis on tryptone semisolid agar (Fig. 2 and Fig. S1). Polar side-chain replacements at any LLF residue abrogated Tsr function, whereas each LLF position tolerated some aliphatic and aromatic amino acid replacements (Fig. 2). These findings suggest that the WT LLF residues contribute to hydrophobic packing interactions that are important for the proper structure and function of the Tsr MH cap.

The LLF residues lie at *d* positions of the Tsr heptad repeats that comprise hydrophobic packing interfaces of the chemoreceptor cytoplasmic domain (Fig. 1). However, S494, the *d* residue in the heptad adjacent to L501, is hydrophilic rather than hydrophobic (Fig. 1*B*). All-codon mutagenesis revealed that, unlike the LLF motif residues, hydrophobic and hydrophilic amino acid replacements at S494 supported chemotaxis (Fig. S1). Only phenylalanine and proline were not tolerated at the residue 494 position, suggesting that there could be a structural transition of some sort between the LLF residues of the MH cap and the remainder of the MH bundle.

To confirm that the signaling defects of LLF* receptors were not a result of changes in their expression or stability, we quantified the steady-state intracellular levels of the mutant receptors by gel electrophoresis and immunoblotting (*Materials and Methods*). All LLF* receptors were present at 0.6–1.6 of the WT Tsr level (Fig. S1). Moreover, Tsr-L508M, the mutant with the lowest expression level, exhibited essentially WT function (Fig. 2*A*), indicating that the functional defects of other LLF* receptors were not simply caused by reduced expression level.

Epistasis and Dominance Tests of LLF* Receptors. To gain insight into the nature of the structural changes caused by LLF* lesions, we asked whether mutant receptors with substantial loss-of-function defects could impair the signaling properties of WT chemoreceptors through epistatic or dominant interactions (32, 34). For epistasis tests, we expressed Tsr-LLF* receptors in a host strain containing WT aspartate receptor (Tar) molecules and examined the cells' ability to carry out serine and aspartate chemotaxis. Tsr and Tar receptors can operate together in mixed trimers of dimers (34–37), but some mutant Tsr receptors can block or “jam” Tar function (i.e., epistasis), whereas others can regain Tsr function (i.e., “rescue”) in mixed trimers (32). For dominance tests, we expressed Tsr-LLF* subunits in host strains containing Tsr subunits that had a recessive lesion (R69E or

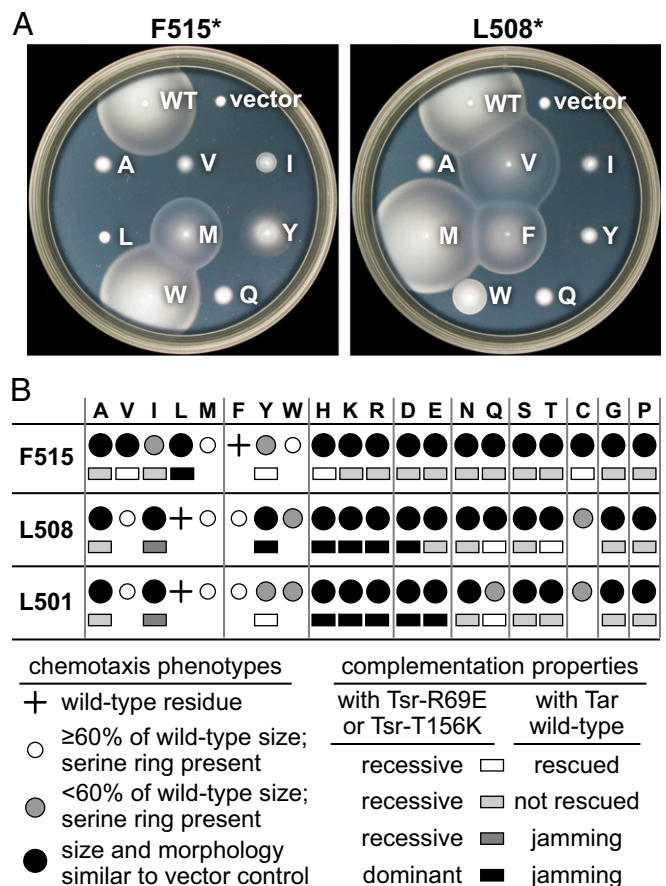


Fig. 2. Functional analysis of Tsr-LLF motif residues. (A) Chemotaxis phenotypes of receptorless host (UU2612; CheR⁺ CheB⁺) carrying plasmid pRR53 derivatives expressing representative Tsr-LLF* mutant receptors with the indicated single amino acid replacements. Tryptone soft agar plates were photographed after incubation for 6 h at 32.5 °C. The WT plasmid was pRR53; the vector control plasmid was pRR48. (B) Chemotaxis phenotypes produced by mutant Tsr receptors with single amino acid replacements at each residue of the LLF motif. Amino acid replacements, grouped by side-chain character, are listed across the top. Mutant receptor performance was assessed on tryptone soft agar as illustrated in A and classified as follows: WT colony diameter and serine ring morphology similar to the WT control (white circles), reduced colony diameter and/or aberrant ring morphology (gray circles), or small colony with no evident serine ring, similar to the vector control (black circles). Complementation properties of the mutant receptors in dominance and epistasis tests are summarized as follows: recessive and rescuable (white rectangles); recessive, not rescuable (light gray rectangles); recessive and jamming (dark gray rectangles); dominant and jamming (black rectangles).

T156K) in the serine-binding domain (16, 33). Heterodimers containing the ligand-binding defect in one subunit and a recessive LLF* lesion in the other subunit will have Tsr function, whereas a dominant LLF* subunit will spoil heterodimer function.

Many of the LLF* mutants proved to have recessive defects (32 of 45), suggesting that their structural alterations were compensated by the corresponding WT residue in a Tsr heterodimer (Fig. 2*B*). However, only a few recessive lesions were functionally rescuable, indicating that mutant Tsr homodimers could not benefit from the presence of WT Tar partners in mixed trimers of receptor dimers (Fig. 2*B*). Some LLF* receptors jammed Tar function; most of those had a basic or acidic side chain at residue L501 or L508 (Fig. 2*B*), whereas corresponding replacements at F515 did not produce epistatic defects (Fig. 2*B*). These functional differences probably reflect the solvent-accessible

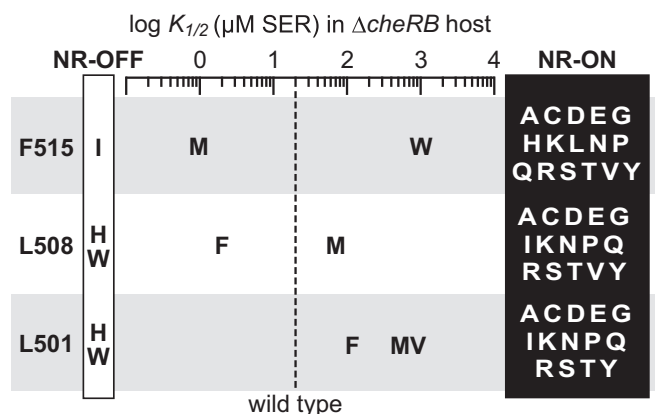


Fig. 3. Signaling properties of Tsr-LLF* receptors in an adaptation-deficient host. Mutant pRR53 derivatives were characterized with *in vivo* FRET kinase assays in receptorless host strain UU2567 (CheR⁻ CheB⁻; *Materials and Methods*). In this strain, WT Tsr produces 50% kinase inhibition in response to ~20 µM serine (broken vertical line). The mutant receptors are indicated with single-letter designations for their amino acid replacements. Mutant receptors that failed to activate CheA were classified as NR and kinase-OFF (i.e., NR-OFF). The majority of LLF mutant receptors elicited CheA kinase activity that could not be inhibited by a serine stimulus (i.e., NR-ON).

location of F515 at the end of the MH cap and the more buried chemical environments of L508 and L501 (Fig. 1).

Signaling Properties of LLF* Receptors. We characterized the ability of mutant receptors to regulate CheA kinase activity in response to serine stimuli with an *in vivo* Förster resonance energy transfer (FRET)-based kinase assay (38, 39). This assay follows CheA autophosphorylation activity, the rate-limiting step in CheY phosphorylation, through a FRET interaction between YFP-tagged CheY and CFP-tagged CheZ, a phosphatase that

preferentially interacts with CheY-P. FRET dose-response data were fitted with a multisite Hill equation, yielding values for serine sensitivity ($K_{1/2}$, the attractant concentration that inhibits 50% of the kinase activity) and for response cooperativity (the Hill coefficient).

We first evaluated LLF* receptors in a strain lacking other receptors and the adaptation enzymes CheR and CheB (UU2567; CheR⁻ CheB⁻). In the absence of adaptation enzymes, the Tsr molecules retain a QEQEE residue pattern at the five modification sites in each subunit: the glutamyl (E) sites are un-methylated; the glutamyl (Q) sites mimic the signaling properties of glutamyl-methyl ester (Em) modifications. In UU2567, most of the LLF* mutants failed to down-regulate CheA activity in response to serine stimuli; the few responsive receptors all had hydrophobic or aromatic replacements (Fig. 3). To determine which LLF* mutants were able to activate the CheA kinase, we subjected cells carrying nonresponsive (NR) receptors to a KCN “stimulus,” which collapses the cellular level of ATP, the phosphodonator for the CheA autophosphorylation reaction. Receptors that activate CheA will respond to KCN with a decrease in the YFP/CFP ratio, providing a measure of their kinase activity in the absence of a traditional attractant response (40). Five NR receptor mutants showed little or no kinase activity in the KCN test (Fig. 3, NR-OFF); all other NR LLF* receptors activated CheA to approximately WT levels (Fig. 3, NR-ON).

Effects of Individual Sensory Adaptation Enzymes on the Signaling Properties of LLF* Receptors. The CheR enzyme acts on receptors in the OFF state and shifts their output toward the ON state by methylating E modification sites (reviewed in refs. 3 and 41). The CheB enzyme recognizes receptors in the ON state and shifts their output toward the OFF state by hydrolyzing Em sites and by deamidating Q sites to E sites. To determine whether the signal outputs of LLF* receptors responded to sensory adaptation enzymes, we conducted FRET experiments in *E. coli* strains containing the modification enzyme most likely to alter the

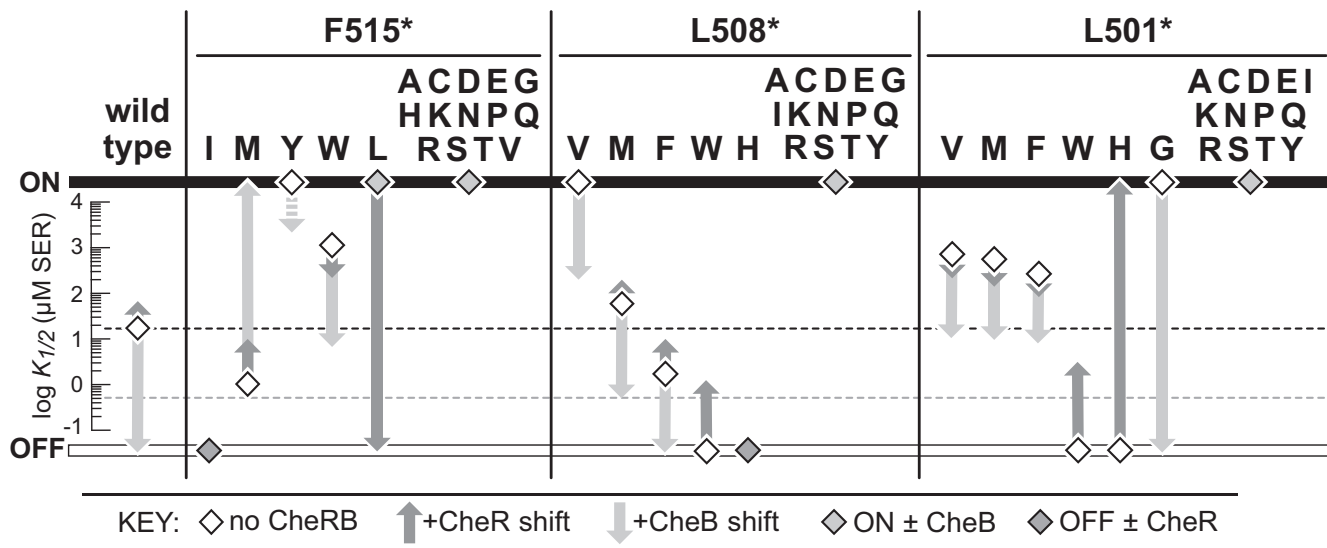


Fig. 4. Signaling properties of Tsr-LLF* receptors in hosts containing a single sensory-adaptation enzyme. Mutant pRR53 derivatives were characterized with *in vivo* FRET kinase assays in receptorless host strain UU2697 (CheR⁺ CheB⁻) and/or strain UU2699 (CheR⁻ CheB⁺; *Materials and Methods*). Horizontal gray and black broken lines respectively indicate the $K_{1/2}$ of WT Tsr in the UU2700 (CheR⁺ CheB⁺) and UU2567 (CheR⁻ CheB⁻) hosts. Diamonds indicate $K_{1/2}$ values of receptors in strain UU2567 (CheR⁻ CheB⁻; Fig. 3); tips of dark gray arrows indicate response values in UU2697 (CheR⁺); tips of light gray arrows indicate response values in UU2699 (CheB⁺). Mutant receptors that exhibited responses in UU2567 (Fig. 3) were tested in UU2697 and UU2699. Receptors with NR-OFF behavior in UU2567 were tested in the UU2697 host; dark gray diamonds indicate no change in behavior. Receptors with NR-ON behavior in UU2567 were tested in the UU2699 host; light gray diamonds indicate no change in behavior. The F515Y receptor exhibited variable high $K_{1/2}$ responses in UU2699 (broken light gray arrow). The F515L and F515M receptors exhibited paradoxical signaling changes (see text): F515L shifted from NR-ON to NR-OFF behavior in the CheR⁺ host (UU2697) and F515M shifted to NR-ON behavior in the CheB⁺ host (UU2699).

output of each mutant receptor: NR-OFF receptors were evaluated in a CheR-containing host (UU2697; CheR⁺ CheB⁻) and NR-ON receptors were evaluated in a CheB-containing host (UU2699; CheR⁻ CheB⁺). All but three of the NR-ON receptors remained kinase-ON and NR in the CheB⁺ host (Fig. 4). Two receptors (F515Y and L508V) became responsive to serine; one (L501G) shifted to NR-OFF behavior. These three receptors are evidently subject to CheB modifications that shift their output toward the kinase-OFF state. Two NR-OFF receptors (L508W, L501W) became responsive to serine in the CheR⁺ host; one (L501H) shifted to NR-ON behavior (Fig. 4). These receptors are evidently subject to CheR modifications that shift their output toward the kinase-ON state. Two mutant receptors (F515I, L508H) remained kinase-OFF and NR in the CheR⁺ host (Fig. 4).

The few LLF* receptors that responded to serine in a host lacking both adaptation enzymes (Fig. 3) were tested in each of the single-enzyme hosts (Fig. 4). The F515W; L508F, M; and L501V, M, F receptors showed little change in behavior in the CheR⁺ host but had enhanced serine sensitivity in the CheB⁺ host. These signaling responses to adaptation enzymes are similar to those of WT Tsr (Fig. 4). In contrast, the F515M receptor shifted to NR-ON behavior in the CheB⁺ host, an inverted output response to CheB modifications.

Adaptational Modification Effects on F515* Receptors. Most LLF* receptors were not able to support chemotaxis in an adaptation-proficient host strain (UU2612; CheR⁺ CheB⁺; Fig. 2), suggesting that they might be defective substrates for one or both of the sensory adaptation enzymes. To explore this issue in greater detail, we compared the signaling properties of selected F515* receptors in an adaptation-proficient FRET host (UU2700; CheR⁺ CheB⁺) vs. their substrate properties for modification in host strains containing one or both of the adaptation enzymes. Adaptational modifications of mutant receptor molecules were detected as mobility shifts in denaturing polyacrylamide gels, as exemplified in Fig. 5C and summarized in Fig. 5B (42–46). Three receptors (F515M, Y, W) that were serine-responsive in UU2700 exhibited WT modification patterns with one or both enzymes (Fig. 5). In contrast, nearly all receptors that were NR-ON in the host lacking adaptation enzymes (UU2567) remained NR and kinase-ON in UU2700. Those tested for modifications (F515A, V, K, D, N, S, G) proved to be very poor substrates for both enzymes (Fig. 5), implying that their MH bundles have a non-native structure. The F515I receptor exhibited NR-OFF behavior in UU2700 and was poorly modified by CheB, but extensively modified by CheR. These properties are consistent with a receptor that is conformationally locked in the native kinase-OFF signaling state. The modification properties of the F515L receptor were nearly identical to F515I, but its signaling behaviors were just the opposite: the adaptation system drove F515L from NR-ON to NR-OFF behavior, despite extensive CheR modifications that should shift Tsr output toward the ON state (Fig. 5). The structural implications of this paradoxical signaling behavior are considered in the *Discussion*.

Suppression Tests of an MH Cap Structural Model. The cytoplasmic domain of Tsr forms an antiparallel four-helix coiled coil with hydrophobic residues at *a* and *d* heptad repeat positions (Fig. 1). The disparity in side-chain volumes at the *a* (V512, A505) and *d* (L501, L508, F515) positions of the MH2 cap helices is a structural feature characteristic of leucine zippers in parallel two-helix coiled coils (47–49). Studies using synthetic peptides and a truncated form of the alphavirus nucleocapsid protein have shown that as few as two leucine residues can form a functional leucine zipper (50, 51). If the L501 and L508 residues adopt a leucine zipper-like structure, the F515 residues would also be well positioned to engage in hydrophobic or aromatic

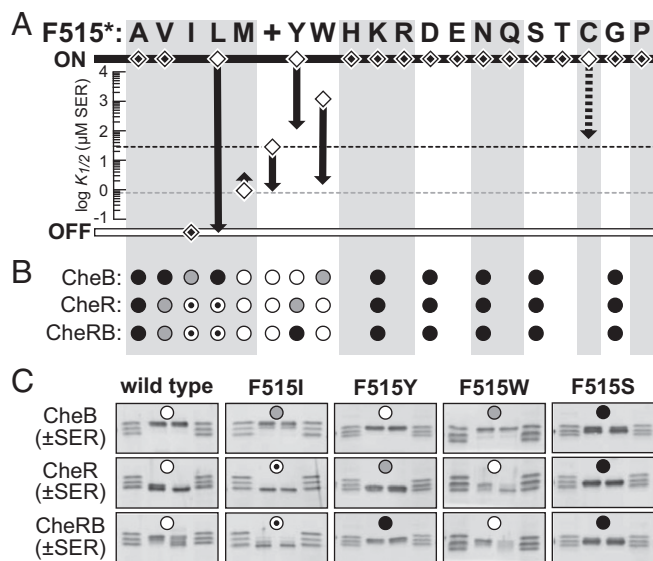


Fig. 5. Signaling and adaptational modification properties of Tsr-F515* mutant receptors. (A) Serine responses produced by mutant receptors in strains UU2567 (CheR⁻ CheB⁻; Fig. 3) and UU2700 (CheR⁺ CheB⁺). WT and mutant plasmid pRR53 derivatives were characterized with in vivo FRET kinase assays (*Materials and Methods*). The broken horizontal black and gray lines respectively indicate the $K_{1/2}$ values for WT Tsr in the UU2567 (white diamond) and UU2700 (black arrowhead) hosts. The response behaviors of most mutant receptors were comparable in the two hosts (white diamonds with a black diamond center). The presence of both adaptation enzymes elicited variable responses by the F515C receptor (broken black arrow). (B) Adaptational modification patterns of Tsr-F515 mutant receptors. Mutant plasmid derivatives were transferred into the following host strains: UU2611 (CheR⁻ CheB⁺), UU2632 (CheR⁺ CheB⁻), and UU2612 (CheR⁺ CheB⁺). Covalent modifications of plasmid-encoded receptor molecules were detected as SDS/PAGE band shifts (*Materials and Methods*). Modification symbols are defined as follows and exemplified in C: white, gray, and black circles respectively designate WT levels of modification, reduced modification, and little or no modification; a black dot inside a white circle designates excessive modification. (C) Examples of mutant receptor modification patterns in the hosts described in B. Outside lanes contain a mixture of 4E, QE, and 4Q Tsr proteins, which are used to determine the modification state of the mutant receptor. The middle two lanes contain the indicated F515* construct in the absence (*Left*) and presence (*Right*) of 10 mM Ser.

stacking interactions (52). A structural model of the Tsr signaling domain from a molecular dynamics (MD) simulation (53) exhibits packing interactions in the MH cap similar to those in leucine zippers (Fig. 6). Notably, interactions between L501–L501' and L508–L508' (Fig. 6A) promote MH2–MH2' packing that is reinforced by potential stacking interactions of F515 and F515' (Fig. 6B).

Because most LLF* mutant receptors were locked in a kinase-ON state, we propose that the LLF motif promotes a zipper-like interaction between the MH2 and MH2' helices that enables Tsr to attain the kinase-OFF output state in response to serine stimuli. Conceivably, LLF* mutants might regain serine responsiveness through a compensatory amino acid change that restores an appropriate MH cap structure or helix-packing stability. To explore this possibility, we selected a variety of L508* and F515* receptors and looked for amino acid replacements at nearby packing residues (V267, V270, V512; Fig. 7A) that could improve their chemotaxis performance on tryptone soft agar plates. Our criteria for positive suppression were (i) that the doubly mutant receptor promote at least 50% of WT performance and (ii) that mutant receptors with either of the individual changes have less function than the doubly mutant receptor. By these criteria, most F515* and L508* mutants could not be suppressed by any amino acid change at V267, V270, or V512 (Fig. 7B).

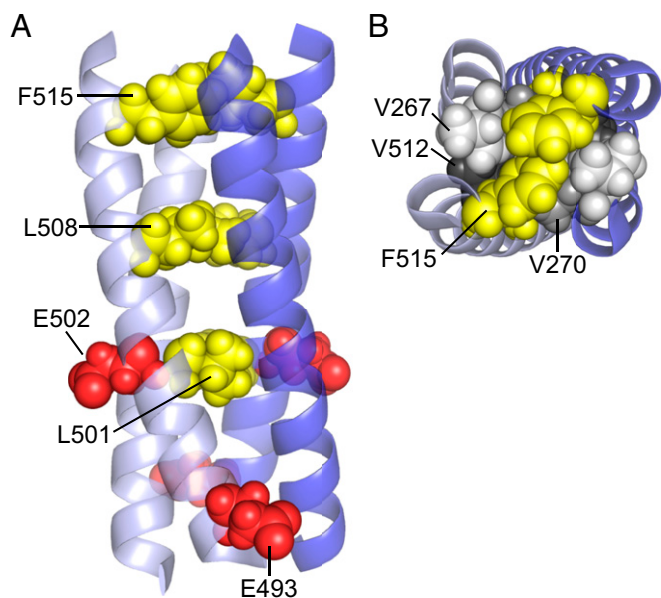


Fig. 6. Structural model of the MH bundle cap. Structures in *A* and *B* represent the final atomic coordinates from a MD simulation of Tsr QE₂EE residues 263–519 (the cytoplasmic signaling domain sans HAMP) (53). (*A*) Side view of the four helices at the MH bundle cap. LLF residues (yellow) and methylation sites E493 and E502 (red) are space-filled. One subunit of the Tsr homodimer is light blue and the other is dark blue. (*B*) End-on (top-down) view of the MH bundle cap. Hydrophobic residues F515 (yellow) and V267 (light gray) lie in the same layer; hydrophobic residues V270 (dark gray) and V512 (black) define the packing layer below.

Two F515 mutants (V, Y) and two L508 mutants (A, I), which retain some hydrophobic character of the WT residues, proved suppressible (Figs. 7*C* and 8*A*). With only one exception (V512C), their suppressors had a large hydrophobic replacement (F, I, L) at the targeted valine residue. Several suppressors (V267L, V270L, V270F) compensated lesions at both F515 and L508 (Fig. 7*C*). Thus, suppression effects were not very allele-specific (Fig. 7*C*), nor were they strictly confined to residues in direct contact in the MH cap structural model (e.g., L508I/V267L; Fig. 7*A*). FRET assays in UU2567 (CheR⁻ CheB⁻) indicated that the functional basis for these suppression effects was a generally additive interaction of the component signaling defects (Fig. 8*B*). The four suppressible receptors had NR-ON behavior; their suppressors all exhibited NR-OFF (V267L; V270F, I; V512C, L) or OFF-shifted (V267F, V270L) signaling properties. Most of the doubly mutant receptors were able to respond to serine with detection sensitivities intermediate to these opposing extremes. Two (L508I/V270L and F515Y/V270I) exhibited NR-ON behaviors in the absence of the adaptational modification system (Fig. 8*B*). There was one exception to this strictly additive rule: the V267F receptor exhibited near-WT serine responsiveness, yet, in combination with F515V, drove its output from NR-ON to NR-OFF (Fig. 8*B*). It seems that rather subtle changes in MH cap helix-packing arrangements and stabilities can produce large shifts in output kinase activity and serine responsiveness.

Absence of the LLF Motif in the Aer Receptor. The *E. coli* Aer receptor is a member of the 36H class of chemoreceptors, yet it does not have the classic type I transmembrane architecture (27) or the LLF heptad residue motif at its MH cap. Instead, Aer has VLL residues at the corresponding LLF positions. To determine whether a Tsr receptor with VLL residues like those in Aer might be functional, we combined the F515L and L501V replacements to

create a doubly mutant receptor. The resulting Tsr-VLL receptor failed to support chemotaxis in soft agar plate assays and was unable to respond to serine in FRET assays, much like the F515L single-mutant receptor (Fig. S2).

Discussion

Signaling Conformations of the Tsr HAMP and MH Bundles. The HAMP structural changes upon signaling are likely to involve shifts in coiled-coil helix-packing interactions (10, 11, 40, 54). In the kinase-OFF state, the HAMP helices probably pack in a canonical *a-d* heptad arrangement of hydrophobic residues, whereas, in the kinase-ON state, they may adopt a less stable arrangement, for example, complementary *x-da* packing. A phase stutter couples the Tsr HAMP and MH bundles in structural opposition such that enhanced helix packing in one element accompanies reduced packing stability in the other (16–19). Signaling-related changes in the HAMP AS2/AS2' helix registers, transmitted through the stutter connection, probably shift the MH1 and MH1' helix registers to modulate the strength of their packing interactions in the MH bundle. According to this view, adaptational modifications should influence the packing arrangements of MH bundle helices in a manner similar to the conformational control by HAMP: CheR-promoted methylation would promote more stable helix packing and ON-shifted output; CheB-promoted demethylation would promote more dynamic packing and OFF-shifted output. State-dependent differences in MH bundle packing stability may also govern the substrate preferences of the adaptation enzymes.

A Zipped-Helix Cap Model of Tsr-HAMP Signaling. Most amino acid replacements at the LLF motif residues lock Tsr output in a kinase-ON state, implying that the native LLF motif enables the

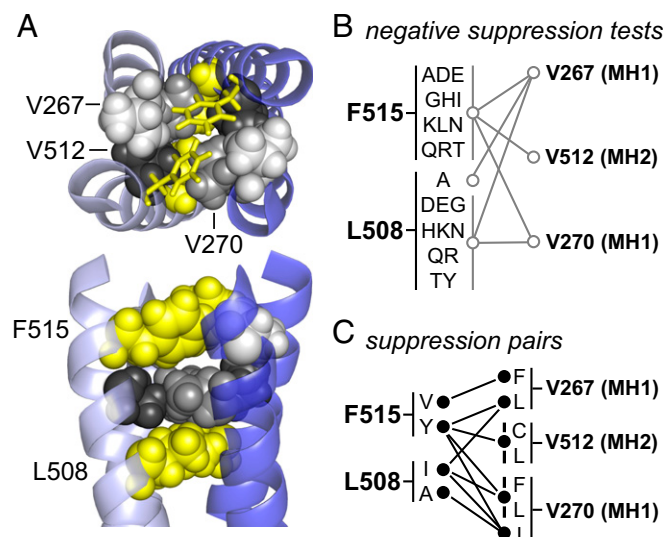


Fig. 7. Second-site suppressors of Tsr-LLF* signaling defects. (*A*) Probable hydrophobic packing partners of LLF residues. Images are from the MD model shown in Fig. 6. (*Upper*) Top-down view of the MH bundle cap. F515 is shown in stick format; its packing partners in the same layer (V267) and adjacent layer (V270, V512) are shown space-filled. (*Lower*) Side view of the F515 and L508 layers and the intervening layer comprised of residues V270 (dark gray) and V512 (black). (*B*) Summary of negative suppression tests. All-codon mutagenesis was carried out individually at codons for V267, V512, and V270 by using Tsr plasmids encoding the F515 or L508 mutants listed on the left. No suppressors were found in these experiments. (*C*) Summary of positive suppression tests. Black lines and circles connect amino acid replacements at F515 and L508 that impair chemotaxis and the amino acid replacements at V267, V512, and V270 that suppressed those chemotaxis defects.

Quantifying Expression of Mutant Tsr Proteins. Assays were performed as previously described (75). Briefly, Tsr proteins were expressed from pRR53 using 100 μ M IPTG in *E. coli* strain UU2610 (CheR⁻ CheB⁻). Cells were grown to midexponential phase, washed, and then resuspended in 2 \times Laemmli sample buffer (76) and boiled for 5 min. Samples were analyzed by SDS/PAGE and immunoblotted with polyclonal rabbit antiserum directed against the highly conserved Tsr signaling domain (77). Quantification was performed with ImageJ (78).

Chemotaxis Assays. Serine chemotaxis performance was assessed on tryptone soft agar plates (79). The receptor-less host strain UU2612 was transformed with Tsr mutant plasmids and individual transformant colonies were picked to tryptone plates containing 0.25% agar, 100 μ M IPTG, and 50 μ g/mL ampicillin. Plates were incubated at 32.5 $^{\circ}$ C for 6–8 h.

Jamming/Rescue and Dominance Tests. Tsr mutant plasmid derivatives were tested in strain UU1623 for ability to block Tar responses (jamming) or to regain Tsr function (rescue) (16). Dominance tests of mutant plasmids were performed in UU2377 and UU2378 (16). Transformant behaviors were scored on tryptone soft agar plates (*Chemotaxis Assays*) containing 50 μ g/mL ampicillin and 0, 50, 100, or 200 μ M IPTG after incubation at 32.5 $^{\circ}$ C for 6–8 h.

Adaptational Modification Assays. Tsr modification tests were performed as previously described (80). Briefly, expression plasmids were transformed into host strains containing CheR alone (R⁺B⁻, UU2632), CheB alone (R⁻B⁺, UU2611), or CheR and CheB together (R⁺B⁺, UU2612). Cells were induced with 100 μ M IPTG, grown to midexponential phase, washed, and then ex-

posed to 10 mM serine for 20 min. Cells were washed again, lysed by boiling in 2 \times Laemmli buffer, and analyzed by SDS/PAGE alongside standard samples containing a 1:1:1 mixture of 4E, QEQE, and 4Q Tsr proteins. Tsr protomers were visualized by immunoblotting.

FRET in Vivo Kinase Assays. A detailed description of the assay and data analysis is presented in ref. 40. Fluorescence signals were collected for CheY-YFP and CheZ-CFP from plasmid pRZ30, along with Tsr constructs from pRR53-based mutant plasmids. The YFP/CFP ratio was calculated, serine responses measured, and data fitted with a multisite Hill equation by using KaleidaGraph 4.5 software (Synergy Software) to obtain $K_{1/2}$ and Hill coefficient values. In the absence of a serine response, kinase activities were calculated from the response to 3 mM KCN (40).

Protein Structure Models. PyMOL (Mac) software was used to construct images from the final coordinates of a 2- μ s MD simulation of the Tsr QEQE signaling domain (53).

ACKNOWLEDGMENTS. We thank Peter Ames for initial characterization of Tsr-F515* mutants, Claudia Studdert for the nonredundant 36H MCP library and for helpful comments on the manuscript, and Lynmarie Thompson for editorial and scientific suggestions that improved the manuscript. This work was supported by a Ruth L. Kirschstein postdoctoral research award F32-GM119355 (to C.E.F.) and National Institute of General Medical Sciences Research Grant GM19559 (to J.S.P.). The Protein-DNA Core Facility at the University of Utah receives support from National Cancer Institute Grant CA42014 to the Huntsman Cancer Institute.

- Bhate MP, Molnar KS, Goulian M, DeGrado WF (2015) Signal transduction in histidine kinases: insights from new structures. *Structure* 23:981–994.
- Zschiedrich CP, Keidel V, Szurmant H (2016) Molecular mechanisms of two-component signal transduction. *J Mol Biol* 428:3752–3775.
- Parkinson JS, Hazelbauer GL, Falke JJ (2015) Signaling and sensory adaptation in *Escherichia coli* chemoreceptors: 2015 update. *Trends Microbiol* 23:257–266.
- Colin R, Sourjik V (2017) Emergent properties of bacterial chemotaxis pathway. *Curr Opin Microbiol* 39:24–33.
- Ames P, Bergman K (1981) Competitive advantage provided by bacterial motility in the formation of nodules by *Rhizobium meliloti*. *J Bacteriol* 148:728–908.
- Fenchel T (2002) Microbial behavior in a heterogeneous world. *Science* 296:1068–1071.
- Caetano-Anollés G, et al. (1988) Role of motility and chemotaxis in efficiency of nodulation by *Rhizobium meliloti*. *Plant Physiol* 86:1228–1235.
- Miller LD, Yost CK, Hynes MF, Alexandre G (2007) The major chemotaxis gene cluster of *Rhizobium leguminosarum* bv. *viciae* is essential for competitive nodulation. *Mol Microbiol* 63:348–362.
- Nilsson M, Rasmussen U, Bergman B (2006) Cyanobacterial chemotaxis to extracts of host and nonhost plants. *FEMS Microbiol Ecol* 55:382–390.
- Hulko M, et al. (2006) The HAMP domain structure implies helix rotation in transmembrane signaling. *Cell* 126:929–940.
- Ferris HU, et al. (2011) The mechanisms of HAMP-mediated signaling in transmembrane receptors. *Structure* 19:378–385.
- Swain KE, Falke JJ (2007) Structure of the conserved HAMP domain in an intact, membrane-bound chemoreceptor: a disulfide mapping study. *Biochemistry* 46:13684–13695.
- Mondéjar LG, Lupas A, Schultz A, Schultz JE (2012) HAMP domain-mediated signal transduction probed with a mycobacterial adenyllyl cyclase as a reporter. *J Biol Chem* 287:1022–1031.
- Watts KJ, Johnson MS, Taylor BL (2011) Different conformations of the kinase-on and kinase-off signaling states in the Aer HAMP domain. *J Bacteriol* 193:4095–4103.
- Airola MV, Watts KJ, Bilves AM, Crane BR (2010) Structure of concatenated HAMP domains provides a mechanism for signal transduction. *Structure* 18:436–448.
- Zhou Q, Ames P, Parkinson JS (2009) Mutational analyses of HAMP helices suggest a dynamic bundle model of input-output signalling in chemoreceptors. *Mol Microbiol* 73:801–814.
- Zhou Q, Ames P, Parkinson JS (2011) Biphasic control logic of HAMP domain signalling in the *Escherichia coli* serine chemoreceptor. *Mol Microbiol* 80:596–611.
- Parkinson JS (2010) Signaling mechanisms of HAMP domains in chemoreceptors and sensor kinases. *Annu Rev Microbiol* 64:101–122.
- Ames P, Zhou Q, Parkinson JS (2014) HAMP domain structural determinants for signalling and sensory adaptation in Tsr, the *Escherichia coli* serine chemoreceptor. *Mol Microbiol* 91:875–886.
- Stewart V (2014) The HAMP signal-conversion domain: static two-state or dynamic three-state? *Mol Microbiol* 91:853–857.
- Stewart V, Chen LL (2010) The S helix mediates signal transmission as a HAMP domain coiled-coil extension in the NarX nitrate sensor from *Escherichia coli* K-12. *J Bacteriol* 192:734–745.
- Wang S (2012) Bacterial two-component systems: Structures and signaling mechanisms. *Protein Phosphorylation in Human Health*, ed Huang C (INTECH, London), Chap 15.
- Hazelbauer GL, Falke JJ, Parkinson JS (2008) Bacterial chemoreceptors: high-performance signaling in networked arrays. *Trends Biochem Sci* 33:9–19.
- Swain KE, Gonzalez MA, Falke JJ (2009) Engineered socket study of signaling through a four-helix bundle: evidence for a yin-yang mechanism in the kinase control module of the aspartate receptor. *Biochemistry* 48:9266–9277.
- Mechaly AE, Sassoon N, Betton JM, Alzari PM (2014) Segmental helical motions and dynamical asymmetry modulate histidine kinase autophosphorylation. *PLoS Biol* 12:e1001776.
- Mechaly AE, et al. (2017) Structural coupling between autokinase and phosphotransferase reactions in a bacterial histidine kinase. *Structure* 25:939–944.e3.
- Zhulin IB (2001) The superfamily of chemotaxis transducers: from physiology to genomics and back. *Adv Microb Physiol* 45:157–198.
- Bibikov SI, Biran R, Rudd KE, Parkinson JS (1997) A signal transducer for aerotaxis in *Escherichia coli*. *J Bacteriol* 179:4075–4079.
- Rebbapragada A, et al. (1997) The Aer protein and the serine chemoreceptor Tsr independently sense intracellular energy levels and transduce oxygen, redox, and energy signals for *Escherichia coli* behavior. *Proc Natl Acad Sci USA* 94:10541–10546.
- Li M, Hazelbauer GL (2011) Core unit of chemotaxis signaling complexes. *Proc Natl Acad Sci USA* 108:9390–9395.
- Alexander RP, Zhulin IB (2007) Evolutionary genomics reveals conserved structural determinants of signaling and adaptation in microbial chemoreceptors. *Proc Natl Acad Sci USA* 104:2885–2890.
- Ames P, Studdert CA, Reiser RH, Parkinson JS (2002) Collaborative signaling by mixed chemoreceptor teams in *Escherichia coli*. *Proc Natl Acad Sci USA* 99:7060–7065.
- Ames P, Zhou Q, Parkinson JS (2008) Mutational analysis of the connector segment in the HAMP domain of Tsr, the *Escherichia coli* serine chemoreceptor. *J Bacteriol* 190:6676–6685.
- Studdert CA, Parkinson JS (2004) Crosslinking snapshots of bacterial chemoreceptor squads. *Proc Natl Acad Sci USA* 101:2117–2122.
- Sourjik V, Berg HC (2004) Functional interactions between receptors in bacterial chemotaxis. *Nature* 428:437–441.
- Lai RZ, et al. (2005) Cooperative signaling among bacterial chemoreceptors. *Biochemistry* 44:14298–14307.
- Li M, Hazelbauer GL (2014) Selective allosteric coupling in core chemotaxis signaling complexes. *Proc Natl Acad Sci USA* 111:15940–15945.
- Sourjik V, Berg HC (2002) Receptor sensitivity in bacterial chemotaxis. *Proc Natl Acad Sci USA* 99:123–127.
- Sourjik V, Vaknin A, Shimizu TS, Berg HC (2007) *In vivo* measurement by FRET of pathway activity in bacterial chemotaxis. *Methods Enzymol* 423:365–391.
- Lai RZ, Parkinson JS (2014) Functional suppression of HAMP domain signaling defects in the *E. coli* serine chemoreceptor. *J Mol Biol* 426:3642–3655.
- Hazelbauer GL, Lai WC (2010) Bacterial chemoreceptors: providing enhanced features to two-component signaling. *Curr Opin Microbiol* 13:124–132.
- Engström P, Hazelbauer GL (1980) Multiple methylation of methyl-accepting chemotaxis proteins during adaptation of *E. coli* to chemical stimuli. *Cell* 20:165–171.
- Sherris D, Parkinson JS (1981) Posttranslational processing of methyl-accepting chemotaxis proteins in *Escherichia coli*. *Proc Natl Acad Sci USA* 78:6051–6055.
- Boyd A, Simon MI (1980) Multiple electrophoretic forms of methyl-accepting chemotaxis proteins generated by stimulus-elicited methylation in *Escherichia coli*. *J Bacteriol* 143:809–815.
- Chelsky D, Dahlquist FW (1980) Structural studies of methyl-accepting chemotaxis proteins of *Escherichia coli*: evidence for multiple methylation sites. *Proc Natl Acad Sci USA* 77:2434–2438.

46. DeFranco AL, Koshland DE, Jr (1980) Multiple methylation in processing of sensory signals during bacterial chemotaxis. *Proc Natl Acad Sci USA* 77:2429–2433.
47. Landschulz WH, Johnson PF, McKnight SL (1988) The leucine zipper: a hypothetical structure common to a new class of DNA binding proteins. *Science* 240:1759–1764.
48. Harbury PB, Zhang T, Kim PS, Alber T (1993) A switch between two-, three-, and four-stranded coiled coils in GCN4 leucine zipper mutants. *Science* 262:1401–1407.
49. Nikolaev Y, Pervushin K (2009) Rethinking leucine zipper – A ubiquitous signal transduction motif. Available at precedings.nature.com/documents/3271/version/1. Accessed May 18, 2017.
50. Burkhard P, Meier M, Lustig A (2000) Design of a minimal protein oligomerization domain by a structural approach. *Protein Sci* 9:2294–2301.
51. Perera R, Owen KE, Tellinghuisen TL, Gorbalenya AE, Kuhn RJ (2001) Alphavirus nucleocapsid protein contains a putative coiled coil alpha-helix important for core assembly. *J Virol* 75:1–10.
52. Martinez CR, Iverson BL (2012) Rethinking the term “pi-stacking”. *Chem Sci (Camb)* 3: 2191–2201.
53. Ortega DR, et al. (2013) A phenylalanine rotameric switch for signal-state control in bacterial chemoreceptors. *Nat Commun* 4:2881.
54. Airola MV, et al. (2013) HAMP domain conformers that propagate opposite signals in bacterial chemoreceptors. *PLoS Biol* 11:e1001479.
55. Coleman MD, Bass RB, Mehan RS, Falke JJ (2005) Conserved glycine residues in the cytoplasmic domain of the aspartate receptor play essential roles in kinase coupling and on-off switching. *Biochemistry* 44:7687–7695.
56. Pedetta A, Massazza DA, Herrera Seitz MK, Studdert CA (2017) Mutational replacements at the “glycine hinge” of the *Escherichia coli* chemoreceptor Tsr support a signaling role for the C-helix residue. *Biochemistry* 56:3850–3862.
57. Koshy SS, Li X, Eyles SJ, Weis RM, Thompson LK (2014) Hydrogen exchange differences between chemoreceptor signaling complexes localize to functionally important subdomains. *Biochemistry* 53:7755–7764.
58. Kashefi M, Thompson LK (2017) Signaling-related mobility changes in bacterial chemotaxis receptors revealed by solid-state NMR. *J Phys Chem B* 121:8693–8705.
59. Bartelli NL, Hazelbauer GL (2015) Differential backbone dynamics of companion helices in the extended helical coiled-coil domain of a bacterial chemoreceptor. *Protein Sci* 24:1764–1776.
60. Bartelli NL, Hazelbauer GL (2016) Bacterial chemoreceptor dynamics: Helical stability in the cytoplasmic domain varies with functional segment and adaptational modification. *J Mol Biol* 428:3789–3804.
61. Samanta D, Borbat PP, Dzikovski B, Freed JH, Crane BR (2015) Bacterial chemoreceptor dynamics correlate with activity state and are coupled over long distances. *Proc Natl Acad Sci USA* 112:2455–2460.
62. Lai RZ, Bormans AF, Draheim RR, Wright GA, Manson MD (2008) The region preceding the C-terminal NWETF pentapeptide modulates baseline activity and aspartate inhibition of *Escherichia coli* Tar. *Biochemistry* 47:13287–13295.
63. Ponder JW, Richards FM (1987) Tertiary templates for proteins. Use of packing criteria in the enumeration of allowed sequences for different structural classes. *J Mol Biol* 193:775–791.
64. Moitra J, Szilák L, Krylov D, Vinson C (1997) Leucine is the most stabilizing aliphatic amino acid in the d position of a dimeric leucine zipper coiled coil. *Biochemistry* 36: 12567–12573.
65. Krylov D, Vinson CR (2001) Leucine zipper. *eLS* (Wiley, New York), pp 1–7.
66. Bibikov SI, Barnes LA, Gitin Y, Parkinson JS (2000) Domain organization and flavin adenine dinucleotide-binding determinants in the aerotaxis signal transducer Aer of *Escherichia coli*. *Proc Natl Acad Sci USA* 97:5830–5835.
67. Taylor BL, Zhulin IB (1999) PAS domains: internal sensors of oxygen, redox potential, and light. *Microbiol Mol Biol Rev* 63:479–506.
68. Watts KJ, Ma Q, Johnson MS, Taylor BL (2004) Interactions between the PAS and HAMP domains of the *Escherichia coli* aerotaxis receptor Aer. *J Bacteriol* 186: 7440–7449.
69. Watts KJ, Johnson MS, Taylor BL (2008) Structure-function relationships in the HAMP and proximal signaling domains of the aerotaxis receptor Aer. *J Bacteriol* 190: 2118–2127.
70. Campbell AJ, Watts KJ, Johnson MS, Taylor BL (2010) Gain-of-function mutations cluster in distinct regions associated with the signalling pathway in the PAS domain of the aerotaxis receptor, Aer. *Mol Microbiol* 77:575–586.
71. Garcia D, Watts KJ, Johnson MS, Taylor BL (2016) Delineating PAS-HAMP interaction surfaces and signalling-associated changes in the aerotaxis receptor Aer. *Mol Microbiol* 100:156–172.
72. Wuichet K, Alexander RP, Zhulin IB (2007) Comparative genomic and protein sequence analyses of a complex system controlling bacterial chemotaxis. *Methods Enzymol* 422:1–31.
73. Parkinson JS, Houts SE (1982) Isolation and behavior of *Escherichia coli* deletion mutants lacking chemotaxis functions. *J Bacteriol* 151:106–113.
74. Gosink KK, Burón-Barral MC, Parkinson JS (2006) Signaling interactions between the aerotaxis transducer Aer and heterologous chemoreceptors in *Escherichia coli*. *J Bacteriol* 188:3487–3493.
75. Mowery P, Ostler JB, Parkinson JS (2008) Different signaling roles of two conserved residues in the cytoplasmic hairpin tip of Tsr, the *Escherichia coli* serine chemoreceptor. *J Bacteriol* 190:8065–8074.
76. Laemmli UK (1970) Cleavage of structural proteins during the assembly of the head of bacteriophage T4. *Nature* 227:680–685.
77. Ames P, Parkinson JS (1994) Constitutively signaling fragments of Tsr, the *Escherichia coli* serine chemoreceptor. *J Bacteriol* 176:6340–6348.
78. Schneider CA, Rasband WS, Eliceiri KW (2012) NIH Image to ImageJ: 25 years of image analysis. *Nat Methods* 9:671–675.
79. Parkinson JS (1976) *cheA*, *cheB*, and *cheC* genes of *Escherichia coli* and their role in chemotaxis. *J Bacteriol* 126:758–770.
80. Slocum MK, Parkinson JS (1985) Genetics of methyl-accepting chemotaxis proteins in *Escherichia coli*: null phenotypes of the *tar* and *tap* genes. *J Bacteriol* 163:586–594.
81. Crooks GE, Hon G, Chandonia JM, Brenner SE (2004) WebLogo: a sequence logo generator. *Genome Res* 14:1188–1190.

Supporting Information

Flack and Parkinson 10.1073/pnas.1721554115

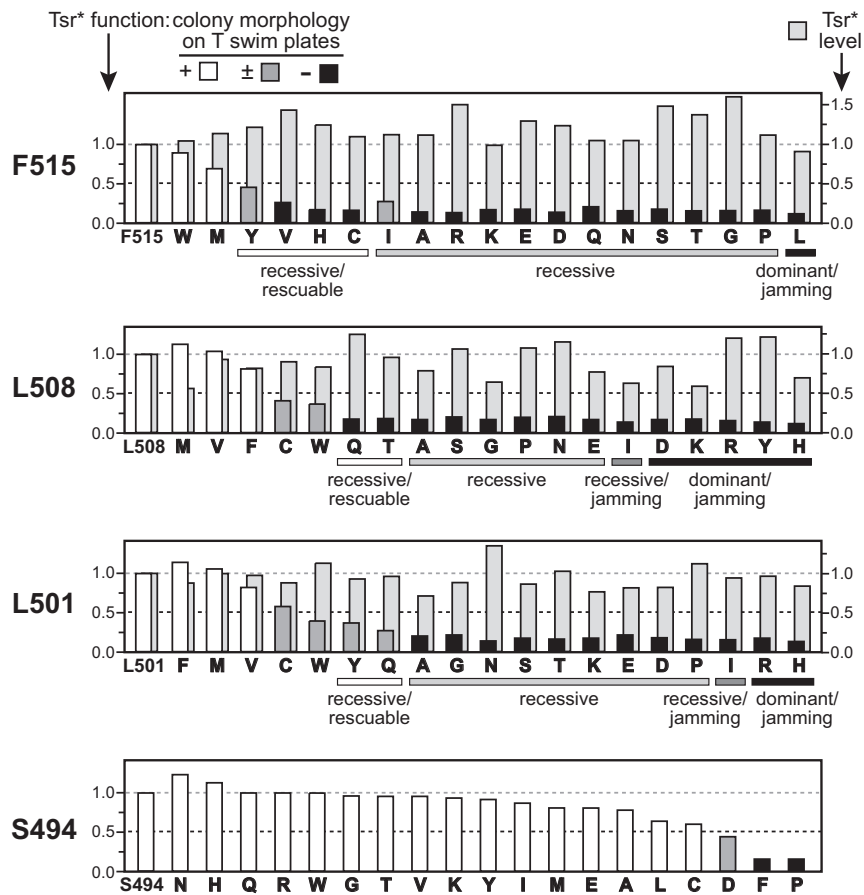


Fig. S1. Chemotaxis phenotypes and expression levels of Tsr-LLF* proteins. Chemotaxis function of mutant plasmids was evaluated in strain UU2612 (CheR⁺ CheB⁺) on tryptone soft agar plates incubated for 5–7 h at 32.5 °C (front histogram bars). Bar shading indicates colony morphology as follows: WT colony diameter and serine ring morphology similar to WT control (white bars); reduced colony diameter and/or aberrant ring morphology (dark gray bars); small colony with no evident serine ring, similar to the vector control (black bars). The steady-state intracellular expression levels of the mutant proteins in strain UU2610 (CheR⁻ CheB⁻) are shown by light gray bars (behind the white, dark gray, or black bars). Shaded horizontal boxes below the upper three panels summarize dominance, jamming, and rescue behaviors as discussed in *Epistasis and Dominance Tests of LLF* Receptors* and Fig. 2.

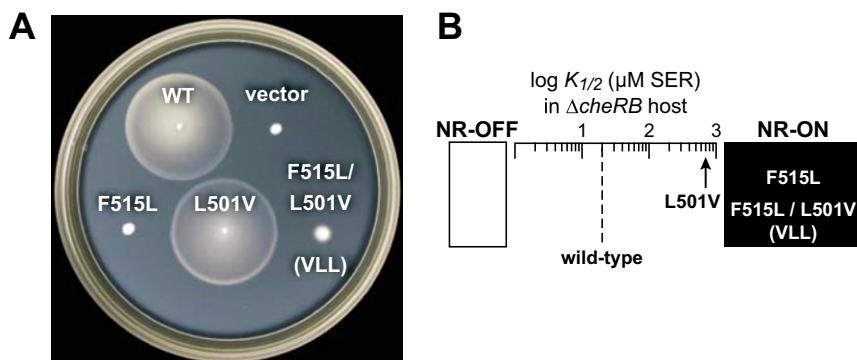


Fig. S2. Chemotactic performance and FRET signaling properties of Tsr-L501V/F515L. These two amino acid replacements mimic the counterparts of the LLF motif residues in the aerotaxis transducer Aer (VLL). (A) Chemotaxis performance of Tsr-F515L, Tsr-L501V, and the F515L/L501V doubly mutant receptor. Plasmid pRR53 derivatives were tested in UU2612 (CheR⁺ CheB⁺) on tryptone soft agar plates incubated for 6 h at 32.5 °C. (B) Signaling properties of Tsr-F515L, Tsr-L501V, and the F515L/L501V doubly mutant receptor. Mutant pRR53 derivatives were characterized with in vivo FRET kinase assays in receptorless host strain UU2567 (CheR⁻ CheB⁻; *Materials and Methods*).

Table S1. Bacterial strains

Strain	Relevant genotype	Ref.
UU1623	<i>tsr</i> Δ7028 <i>tap</i> Δ3654 <i>trg</i> Δ100	1
UU2377	<i>tsr</i> -R69E <i>aer</i> Δ1 (<i>tar</i> - <i>tap</i>)Δ5201 <i>trg</i> Δ4543 Δ(<i>recA</i>)	1
UU2378	<i>tsr</i> -T156K <i>aer</i> Δ1 (<i>tar</i> - <i>tap</i>)Δ5201 <i>trg</i> Δ4543 Δ(<i>recA</i>)	1
UU2567	(<i>tar</i> - <i>cheZ</i>)Δ4211 <i>tsr</i> Δ5547 <i>aer</i> Δ1 <i>trg</i> Δ4543 (<i>cheY</i> - <i>cheZ</i>)Δ1215	2
UU2610	(<i>tar</i> - <i>cheB</i>)Δ4346 <i>tsr</i> Δ5547 <i>aer</i> Δ1 <i>trg</i> Δ4543	3
UU2611	(<i>tar</i> - <i>cheR</i>)Δ4283 <i>tsr</i> Δ5547 <i>aer</i> Δ1 <i>trg</i> Δ4543	3
UU2612	(<i>tar</i> - <i>tap</i>)Δ4530 <i>tsr</i> Δ5547 <i>aer</i> Δ1 <i>trg</i> Δ4543	3
UU2632	<i>cheB</i> Δ4345 (<i>tar</i> - <i>tap</i>)Δ4530 <i>tsr</i> Δ5547 <i>aer</i> Δ1 <i>trg</i> Δ4543	3
UU2697	<i>cheB</i> Δ4345 (<i>tar</i> - <i>tap</i>)Δ4530 <i>tsr</i> Δ5547 <i>aer</i> Δ1 <i>trg</i> Δ4543 (<i>cheY</i> - <i>cheZ</i>)Δ1215	2
UU2699	(<i>tar</i> - <i>cheR</i>)Δ4283 <i>tsr</i> Δ5547 <i>aer</i> Δ1 <i>trg</i> Δ4543 (<i>cheY</i> - <i>cheZ</i>)Δ1215	2
UU2700	(<i>tar</i> - <i>tap</i>)Δ4530 <i>tsr</i> Δ5547 <i>aer</i> Δ1 <i>trg</i> Δ4543 (<i>cheY</i> - <i>cheZ</i>)Δ1215	2

- Zhou Q, Ames P, Parkinson JS (2009) Mutational analyses of HAMP helices suggest a dynamic bundle model of input-output signalling in chemoreceptors. *Mol Microbiol* 73:801–814.
- Lai RZ, Parkinson JS (2014) Functional suppression of HAMP domain signaling defects in the *E. coli* serine chemoreceptor. *J Mol Biol* 426:3642–3655.
- Zhou Q, Ames P, Parkinson JS (2011) Biphasic control logic of HAMP domain signalling in the *Escherichia coli* serine chemoreceptor. *Mol Microbiol* 80:596–611.